

ARTICLE

Bonding characteristic and electronic property of $\text{TiC}_x\text{N}_{1-x}(001)/\text{TiC}(001)$ interface: A first-principles study

Xingwen Fan,^{b)} Song Wang,^{b)} Xianfeng Yang, and Guoli Ni

College of Material Science and Engineering, Southwest Jiaotong University, Chengdu 610031, China

Jingyi Zhang

Science and Technology on Advanced Functional Composites Laboratory, Aerospace Research Institute of Materials & Processing Technology, Beijing 100076, China

Da Li^{a)}

College of Material Science and Engineering, Southwest Jiaotong University, Chengdu 610031, China

(Received 10 January 2018; accepted 22 March 2018)

The $\text{TiC}_x\text{N}_{1-x}(001)/\text{TiC}(001)$ interface was studied by the first-principles method to provide the theoretical basis for developing $\text{TiC}_x\text{N}_{1-x}/\text{TiC}$ coatings. The partial density of state (PDOS), charge density, charge density difference, and Mulliken population analysis were utilized to investigate the bonding nature and the electronic characteristic of the $\text{TiC}_{0.25}\text{N}_{0.75}/\text{TiC}$ interface. The corresponding results indicate that the bonding nature at the interface is ionic and covalent characteristics, which also exist in bulk materials. The extreme similarity of PDOS among interfacial C, N, and Ti atoms and their bulk counterparts reveals that the electronic structure transition at the interface is smooth. The results of Mulliken population analysis and plots of charge density and charge density difference demonstrate that the charge increased for C in the TiC side is less than that for N in the $\text{TiC}_{0.25}\text{N}_{0.75}$ side, which reveals that the ionic bond in $\text{TiC}_{0.25}\text{N}_{0.75}$ is stronger than that in TiC. Therefore, $\text{TiC}_{0.25}\text{N}_{0.75}$ coating can be an alternative choice to combine with TiC coating in the actual production process of multilayer coatings.

I. INTRODUCTION

TiC as transition-metal carbides¹ is widely utilized as coating materials because of its unique properties, including high melting point, low density, high hardness, superior thermal conductivity, chemical stability, and wear resistance.^{2–4} Besides, $\text{Ti}(\text{C}_x\text{N}_{1-x})$, a solid solution of TiC and TiN,⁵ also displays excellent properties as coatings.⁶ Especially, compared with monolayer coatings, some properties such as microhardness and wear resistance of multilayer coatings can be improved obviously.^{7,8} What is more, multilayer coatings also show better adhesion properties than monolayer coating on the steel substrate.⁹ Meanwhile, more interfaces of multilayer coatings can decrease the pores and other defects which normally exist in the monolayer coating.^{10–12} Therefore, further study of multilayer coatings is extremely meaningful.

Nowadays, many researchers focus on TiC and Ti(CN) solid solution multilayer coatings.^{12,13} Notably, the TiCN/TiC material system, one of the important composite coatings with high hardness, better anti-abrasive capability, and good wear resistance, is widely accepted

as a coating material for high-speed cutting tools and mechanical components.^{14–17} Zhang et al.¹² used the chemical vapor deposition (CVD) method to manufacture TiC/Ti(CN)/TiN multilayer coatings on different high-strength steels, who found that the coatings prepared by CVD not only own high adhesion and hardness but also provide good resistance for chloride-ion corrosion. Besides, they also fabricated Ti(CN) multilayer coatings on 35CrMo steel and discovered that the coatings containing $\text{TiC}_{0.2}\text{N}_{0.8}$ possess favourable mechanical properties.¹⁸ Yasuoka et al.¹⁷ compared the mechanical performance of $\text{TiC}_x\text{N}_{1-x}$ single-layer coating with that of the $\text{TiC}_x\text{N}_{1-x}$ multilayer. They obtained that the abrasion resistance of multilayer coatings is better than single-layer coating and the $\text{TiC}_x\text{N}_{1-x}$ with 10–30% C displays the best. Though the experiments can obtain good results and phenomena, the investigation on microscopic and mechanical properties is difficult by using experimental methods.

In fact, the properties of coatings are closely related with their electronical and interfacial structure.^{19–21} First-principles calculation on TiC and Ti(CN) coatings has been verified to be an effective method to study the electronical structure. Zaoui et al.²² discussed the electronic properties of $\text{TiC}_x\text{N}_{1-x}$, who found that the total density of state (DOS) of $\text{TiC}_x\text{N}_{1-x}$ is hybridized by C(N) *s* or *p* states and Ti *d*-states. Kim et al.⁵ who used

^{a)}Address all correspondence to this author.

e-mail: hardfacing@home.swjtu.edu.cn

^{b)}These authors contributed equally to this work.

DOI: 10.1557/jmr.2018.79

first-principles calculation studied the phase stability of $\text{TiC}_{1-x}\text{N}_x$ with different temperatures and draw a conclusion that with the increasing temperature, nitrogen-rich phases became less stable. Li et al.²³ indicated that the stacking of interfacial atoms has an influence on bonding nature, charge transfer and distribution, which will affect interface mechanical properties. Meanwhile, interface fracture toughness can straightforwardly be evaluated by adhesion energy, a parameter affected by interfacial atom species and the total energy of the interface structure. Guo et al.¹⁹ studied the tensile and shear deformations of the interface using the first-principles calculations and pointed out that the tensile and shear deformation can be accommodated by a typical metallic bonding characteristics.

However, few literature studies investigate on the interface structure of $\text{TiC}_x\text{N}_{1-x}/\text{TiC}$ multilayer coatings.

On the one hand, local bonding, specific atomic structure, and local chemistry at the interface would affect the properties of $\text{TiC}_x\text{N}_{1-x}/\text{TiC}$ multilayer coatings but few experimental methods can effectively study it. On the other hand, calculations on the $\text{TiC}_x\text{N}_{1-x}/\text{TiC}$ interface are more difficult and challenging. In our previous work, we have calculated the $\text{TiC}(111)/\text{TiN}(111)$ interface in the early stage and found that the interface covalent and ionic bond play a major role for the interface properties.²⁴ To complete description of our work, the interfacial properties of $\text{TiC}_x\text{N}_{1-x}(001)/\text{TiC}(001)$ are investigated by first-principles calculation, which includes the interfacial atomic structure, interfacial ideal work of adhesion, and their charge distribution. Based on the calculated results, we want to understand the effect of interface doping on the interface properties and propose some useful advice for design and investigate multilayer coatings.

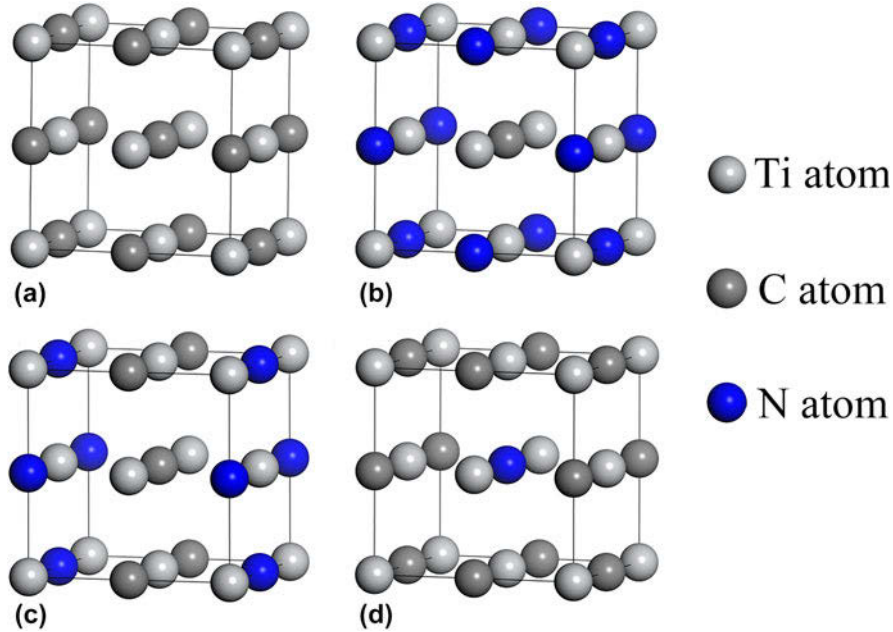
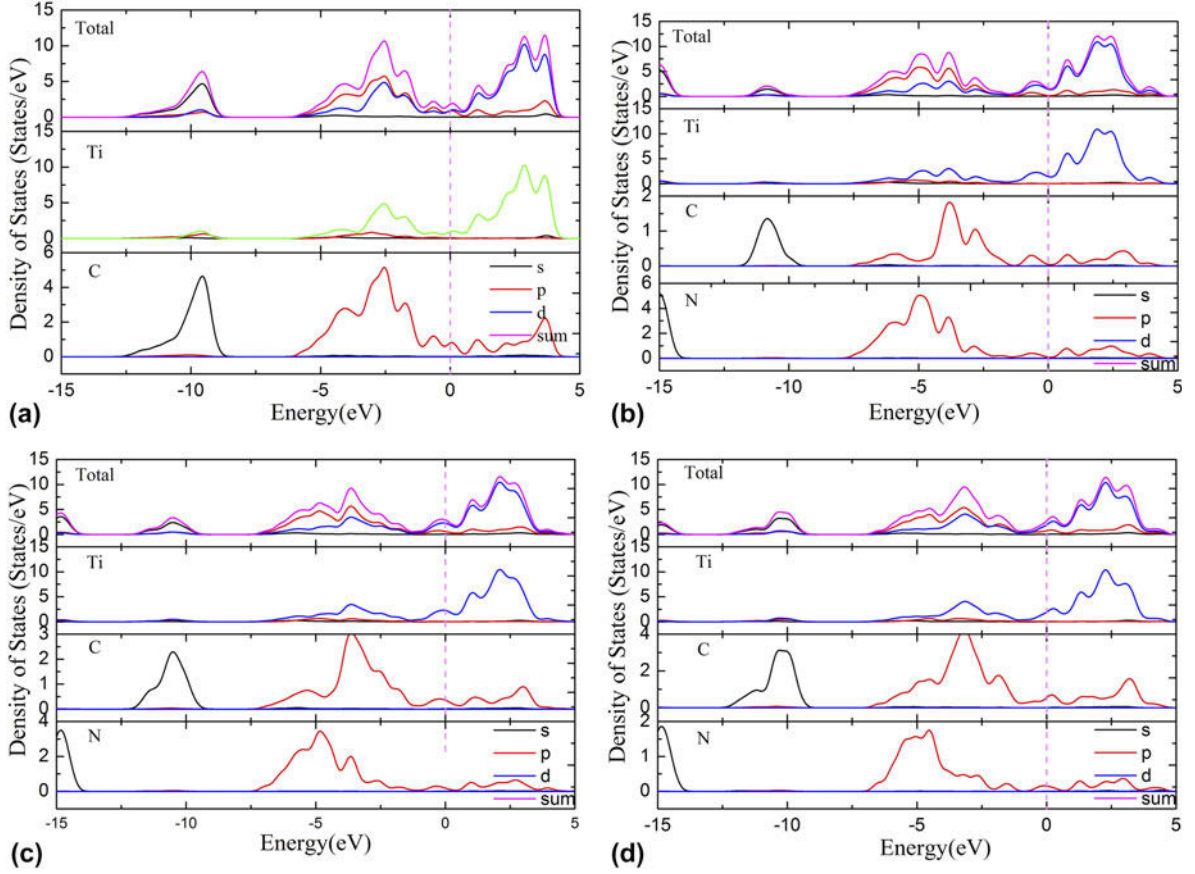


FIG. 1. Crystal structures of (a) TiC , (b) $\text{TiC}_{0.25}\text{N}_{0.75}$, (c) $\text{TiC}_{0.5}\text{N}_{0.5}$, and (d) $\text{TiC}_{0.75}\text{N}_{0.25}$.

TABLE I. Calculated and experimental (Exp.) values of the properties of all structures.

Structure	Method	Lattice constants a (\AA)	Bulk modulus B_0 (GPa)	Formation energies ΔE_f (eV)
TiC	This work	4.33	226	-0.91
	Other work	4.33 ²⁷	249 ²⁷	-0.89 ²⁷
	Exp.	4.33 ²⁸	242 ²⁸	-0.78 ²⁹
$\text{TiC}_{0.25}\text{N}_{0.75}$	This work	4.27	261	-1.71
	Other results	4.27, ¹ 4.25 ²⁵	268, ⁵ 275 ²⁵	...
	Exp.	4.27 ³⁰
$\text{TiC}_{0.5}\text{N}_{0.5}$	This work	4.29	246	-1.45
	Other results	4.28, ¹ 4.28 ²⁵	264, ⁵ 269 ²⁵	...
	Exp.	4.28 ³⁰
$\text{TiC}_{0.75}\text{N}_{0.25}$	This work	4.31	240	-1.19
	Other results	4.31, ¹ 4.30 ²⁵	259, ⁵ 251 ²⁵	-1.19 ²⁶
	Exp.	4.30 ³⁰

FIG. 2. Total and PDOS for all bulks (a) TiC , (b) $\text{TiC}_{0.25}\text{N}_{0.75}$, (c) $\text{TiC}_{0.5}\text{N}_{0.5}$, and (d) $\text{TiC}_{0.75}\text{N}_{0.25}$. The E_{F} is set to zero.

II. COMPUTATIONAL DETAILS

Cambridge sequential total energy package based on density functional theory was used in this paper. Generalized gradient approximation (GGA) of Perdew–Burke–Ernzerhof (PBE) was utilized to address exchange-correlation function. Subsequently, to test the accuracy of parameters utilized in this paper, the bulk properties of TiC and $\text{TiC}_x\text{N}_{1-x}$ ($0 < x < 1$) were calculated. Meanwhile, the surface properties of all slabs with different layer numbers were discussed to gain the suitable layer numbers of bulk-like slabs used for the following interface structure calculation. The plane-wave cutoff energy in this work is 320 eV for all bulks, surfaces, and interfaces. Sampling of the irreducible edge of the Brillouin zone was carried out with the regular Monkhorst–Pack k -point grid. $6 \times 6 \times 6$ k -point mesh is used for both bulks and $9 \times 9 \times 1$ k -point mesh is utilized for the surfaces and interfaces. For the convergence tolerances, the maximum force, maximum displacement, and the energy are set as 0.03 eV/ \AA , 0.001 \AA , and 1×10^{-5} eV/atom, respectively. A vacuum of 10 \AA for surfaces and a vacuum of 25 \AA for interfaces were added respectively, which can avoid unexpected interaction with the periodic cell structure.

TABLE II. The test results for surface convergence with different methods. The (A) part is the results for surface energy convergence with respect to slab thickness, and part (B) is the results of the spacing changes after the $\text{TiC}(001)$ surface relaxations (the percentage increase or decrease of the layer spacing is presented as Δ_{ij}).

(A)	Atomic layer	Number of layers (n)				
		1	3	5	7	9
	δ (J/m ²)	2.17	1.61	1.54	1.50	1.50

(B)	Species	Interlayer spacing	Number of layers (n)			
			3	5	7	9
C		Δ_{12}	1.71	1.66	1.79	1.98
		Δ_{23}	...	0.13	0.18	0.20
		Δ_{34}	0.15	0.10
		Δ_{45}	0.98
Ti		Δ_{12}	-3.51	-2.81	-2.66	-2.40
		Δ_{23}	...	-1.05	-1.17	-0.75
		Δ_{34}	-0.99	-0.10
		Δ_{45}	-0.17

III. BULK AND SURFACE PROPERTIES

A. Bulk properties

All the optimized structures of $\text{TiC}_x\text{N}_{1-x}$ are shown in Fig. 1. Due to TiC and TiN belong to the NaCl-type

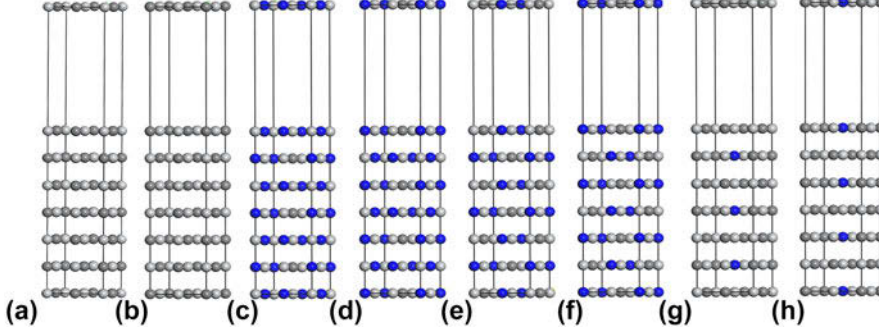


FIG. 3. Plots of $E_{\text{TiC}_x\text{N}_{1-x}(001)}$ with 7 layers of atoms (a) first termination structure of TiC, (b) second termination structure of TiC, (c) first termination structure of $\text{TiC}_{0.25}\text{N}_{0.75}$, (d) second termination structure of $\text{TiC}_{0.25}\text{N}_{0.75}$, (e) first termination structure of $\text{TiC}_{0.5}\text{N}_{0.5}$, (f) second termination structure of $\text{TiC}_{0.5}\text{N}_{0.5}$, (g) first termination structure of $\text{TiC}_{0.75}\text{N}_{0.25}$, and (h) second termination structure of $\text{TiC}_{0.75}\text{N}_{0.25}$.

structure, all the $\text{TiC}_{1-x}\text{N}_x$ ($0 < x < 1$) use the same structure.²⁵

To test the rationality of parameters utilized, some parameters of all bulks including lattice constant, bulk modulus, and formation energy were calculated by using the GGA-PBE method. The calculated results in this work were compared with those of experiments and other published papers, which are listed in Table I. What is worth mentioning that formation energy can be calculated by Eq. (1)²⁶

$$\Delta E_f(\text{TiC}_m\text{N}_n) = \frac{E_{\text{TiC}_m\text{N}_n} - E_{\text{Ti}} - mE_{\text{C}} - nE_{\text{N}}}{1 + m + n} , \quad (1)$$

where $E_{\text{TiC}_m\text{N}_n}$ is the total energy for TiC_mN_n , E_{Ti} is the total energy per atom of Ti bulk crystal, and E_{C} and E_{N} are the total energy of a single C and N structure.

The calculated lattice constants ‘ a ’, bulk modulus ‘ B_0 ’, and formation energies of all structures shown in Fig. 1 are listed in Table I. Notably, the relevant calculated results of $\text{TiC}_x\text{N}_{1-x}$ in this work coincide well with other previously published results, which demonstrate that the parameters utilized in this paper are reasonable and accurate.

The partial density of state (PDOS) of TiC and $\text{TiC}_x\text{N}_{1-x}$ structures is calculated, as shown in Fig. 2. Due to the similar structure, the PDOS of all bulks are similar. One obvious feature is that next to the Fermi level (E_F), the DOS for all structures exist in the form of $p-d$ hybridization formed by p states of N and C and d states of Ti, which generates a shear-resistive covalent bonding caused by nonmetal $2p$ and metal d electrons coupling. What is more, the DOS of all bulk materials at the Fermi level consists of peaks, which demonstrates metallic characteristics. That is, the bond of these materials is not a single one, which contains metallic bonding and covalent bonding.

B. Surface convergence analysis

First of all, surface structures are studied to investigate the microscopic properties of the $\text{TiC}_x\text{N}_{1-x}/\text{TiC}$ interface.

TABLE III. The adhesion energy, W_{ad} (J/m²), of 12 interface structures after relaxation.

		$\text{TiC}_{0.25}\text{N}_{0.75}$		$\text{TiC}_{0.5}\text{N}_{0.5}$		$\text{TiC}_{0.75}\text{N}_{0.25}$	
		A	B	A	B	A	B
TiC	A	0.01	4.10	-1.81	4.14	-2.74	4.31
	B	3.99	0.09	-1.44	-0.94	4.55	-0.94

It is obvious that both sides of slabs must be thick enough to present bulk-like characteristic interiors. To obtain the suitable minimum numbers of the layer, there are two methods widely utilized. One method is to verify the convergence of surface energy by increasing atom layers. The other method is that the increase or decrease of the layer spacing is tested by increasing atom layers.³¹ Surface energy (δ) is used to describe the surface stability, which is the energy required to split the crystal into two parts along a plane. The surface energy (δ) can be obtained by Eq. (2).²⁸

$$\delta = [E_{\text{slab}}(N) - NE_{\text{bulk}}]/2A , \quad (2)$$

where $E_{\text{slab}}(N)$ is the total energy of surface supercell slab, N is the total number of atoms in the slab, E_{bulk} is the total energy per atom in the bulk, and A is the surface area.

Obviously, it can be seen in the part (A) of Table II that the surface energy for the TiC(001) surface converges rapidly with increasing slab thickness to 1.50 J/m² when the layers of slab exceed 5 layers. The results of this work are consistent with those of other ones.^{32,33} Therefore, a 7-layer slab of TiC(001) is selected for further study. Meanwhile, given the similar structure of these 4 materials, the 7-layer slab of 4 materials is chosen to investigate the electronic structure.

For further verification of the suitable minimum numbers of the layer, the convergence test is performed with the second method which is to test the layer distance changes of the TiC(001) surface by increasing atom layers, and the results of the spacing changes are listed

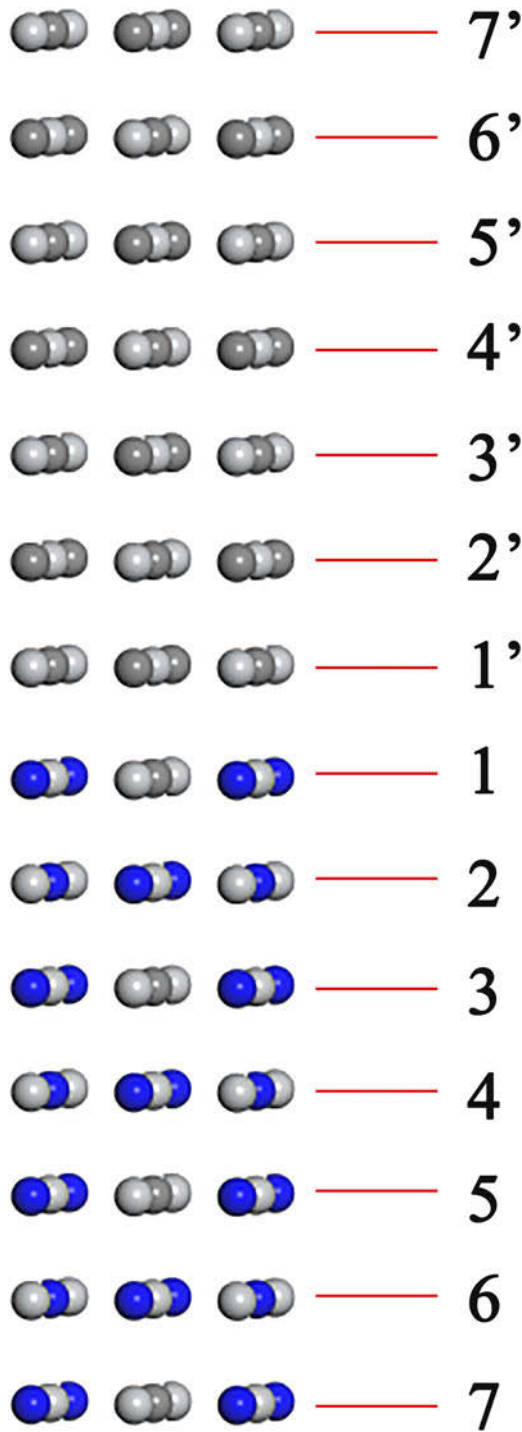


FIG. 4. Plot of the first terminated structure of TiC contacting with second terminated structure of $\text{TiC}_{0.25}\text{N}_{0.75}$.

in the part (B) of Table II, where the percentage increase or decrease of the layer spacing is presented as Δ_{ij} , and n is the number of layers. From the part (B) of Table II, the changes of the layer distance decrease gradually after the structures are relaxed. From the changes of atomic spacing from surfacial atom layers to deeper atom layers

in TiC, the relaxation of the TiC structure mainly occurs in the top 3 atomic layers. It can be easily obtained that the top 3 interlayer relaxations for the (001) plane is converged with the increasing number of layers. When the number of layer exceeds 5, convergence of the top 3 layers occurs. Therefore, 7-layer surface structures for all TiC and $\text{TiC}_x\text{N}_{1-x}$ can effectively represent the bulk characteristic of the slab.

Meanwhile, Fig. 3 shows the 7-layer surface structures for $\text{TiC}_x\text{N}_{1-x}$, which is added a vacuum of 10 Å. One feature can be observed that the surface structure of every material can be divided into 2 terminated structures.

IV. INTERFACE PROPERTIES OF $\text{TiC}_x\text{N}_{1-x}(001)$ AND $\text{TiC}(001)$

To determine the most stable interface theoretically, the ideal work, the adhesion energy W_{ad} , which can effectively predict the mechanical properties of an interface, is calculated. The adhesion energy is expressed not only as the reversible energy needed to separate the interface into two free surfaces but also the difference in total energy between the relevant isolated slabs and interface. The adhesion energy can be gained by Eq. (3).³⁴

$$W_{\text{ad}} = (E_{\text{TiC}_x\text{N}_{1-x}} + E_{\text{TiC}} - E_{\text{IF}})/A \quad , \quad (3)$$

where the $E_{\text{TiC}_x\text{N}_{1-x}}$, E_{TiC} , and E_{IF} are the total energy of the isolated $\text{TiC}_x\text{N}_{1-x}$ slab, TiC slab, and $\text{TiC}_x\text{N}_{1-x}$ interface, respectively. A is the interface area.

Due to every $\text{TiC}_x\text{N}_{1-x}$ has two terminated structures mentioned in Fig. 3, a total of 12 interface structures of $\text{TiC}_x\text{N}_{1-x}(001)/\text{TiC}(001)$ are obtained.

The adhesion energy results of all interface structures after relaxation are listed in Table III where A presents the first terminated structure of TiC and $\text{TiC}_x\text{N}_{1-x}$ while B presents the second terminated structure of TiC and $\text{TiC}_x\text{N}_{1-x}$. It can be seen that the value of adhesion energy of $\text{TiC}_{0.25}\text{N}_{0.75}(001)/\text{TiC}(001)$ interface structures is positive, which reflect that all interface structures are stable. For all interface structures, the biggest adhesion energy always occurs at the interface of the first structure of TiC and second structure of $\text{TiC}_x\text{N}_{1-x}$ or second structure of TiC and first structure of $\text{TiC}_x\text{N}_{1-x}$, which can be explained that the existence of the interface would not break the continuity of each bulk internal structure. The value of adhesion energy that is negative reflects that the corresponding interface is unstable. Therefore, the interface of TiC first terminated structure combining $\text{TiC}_{0.25}\text{N}_{0.75}$ second terminated structure (shown in Fig. 4) is chosen for further study.

To further study the bonding mechanism of $\text{TiC}_{0.25}\text{N}_{0.75}(001)$ and $\text{TiC}(001)$ interfaces, the PDOS of which was calculated, as shown in Fig. 5. The first layer is closer to the interface and the 7th layer is the surface away from the interface.

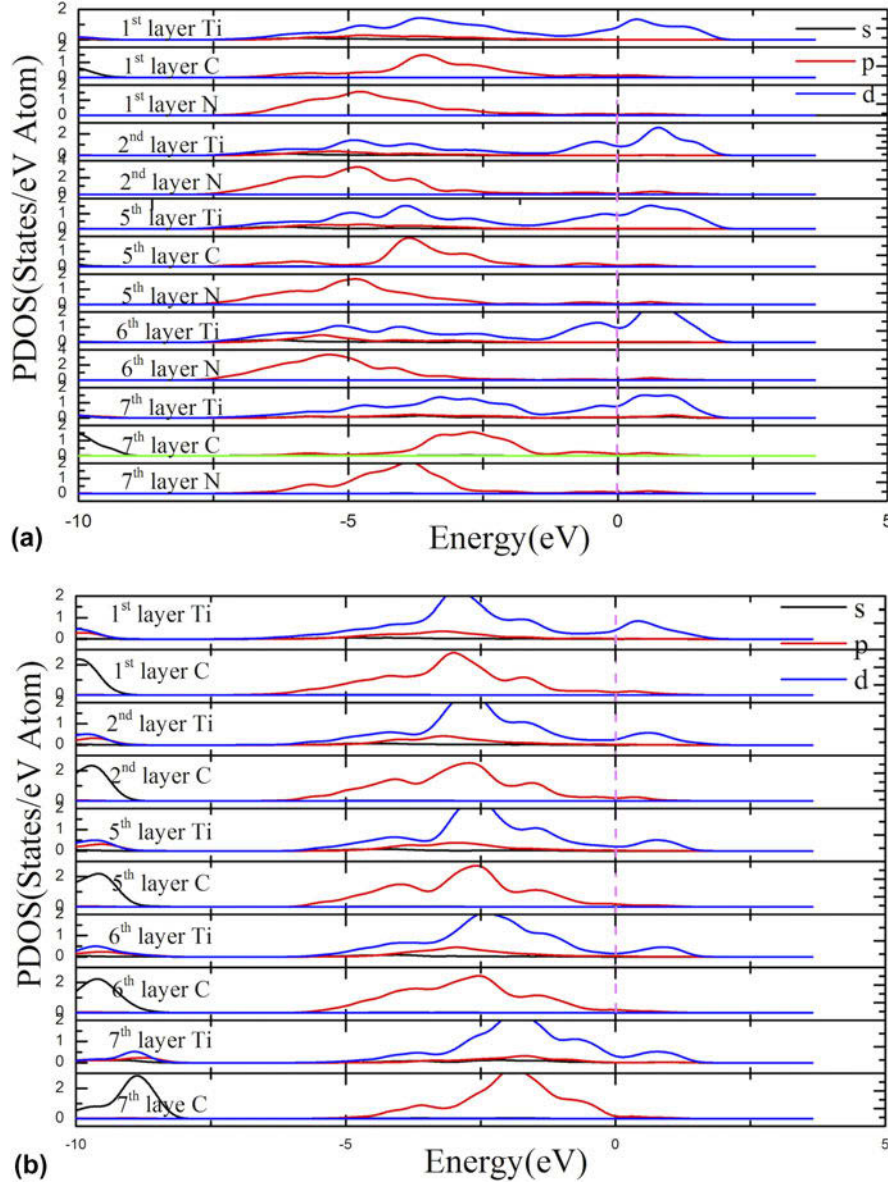


FIG. 5. DOS projected on the selected interface after relaxation. The first layer is closer to the interface. The top figure (a) presents the PDOS of $\text{TiC}_{0.25}\text{N}_{0.75}$ layers and the bottom one (b) shows those of TiC layers. The E_F is set to zero denoted by a dash line.

From Fig. 5, it can be seen that the states at E_F of all layers are mainly consist of Ti d state and consist of prominent peaks, which indicate that $\text{TiC}_{0.25}\text{N}_{0.75}$ and TiC possess metallic characteristics. In addition, the important hybridization of Ti d and C (N) p states below and at E_F demonstrates the formation of covalent bonding. Moreover, the extreme similarity of the PDOS between interfacial C, N, and Ti atoms and their bulk counterparts reveals that the electronic structure transition at the interface from $\text{TiC}_{0.25}\text{N}_{0.75}$ to TiC is smooth. By contrast, the PDOS for surface C and N of $\text{TiC}_{0.25}\text{N}_{0.75}$ (7th layer) is visibly different from that for C and N away from interface (5th layer). On the one hand, the whole characteristic of the PDOS for surface C and N (7th layer)

exists an obvious movement to valence band direction. On the other hand, the PDOS of surface C and Ti in TiC (7th layer) is different from that of C and Ti in TiC bulk. What is more, the 6th layer Ti and 6th layer N are similar with internal layers of Ti and N (away from the surface), which demonstrates that the surface effect affects only one or two atomic layers.

Although covalent bonding information is revealed by DOS, the related information of ionicity and electron transfer can be clearly obtained by the plots of charge density and charge density difference along the (010) plane, as shown in Fig. 6. The reason why the (010) plane for the interface is chosen is that the slice passes through C, Ti, and N atoms at the interface,

which is easy to observe the bonding interaction at the interface.

It can be seen from Fig. 6 that the bonds are clearly generated among Ti, N, and C atoms. The charge density distributions of interfacial Ti–C atoms and Ti–C atoms away from the interface are extremely similar, which can be explained due to the continuity of the atomic structure. Moreover, one characteristic is the visible charge distortion between interfacial C and Ti as well as N and Ti. All of these show that the interfacial bonding is ionic and covalent. Furthermore, the charge transfer among the neighbor Ti, C, and N atoms can be observed. The charge depletion region is existed near the Ti atom while the region of charge obtaining is existed near the C or N atom, which indicates that some electrons have been transferred from Ti atom to C or N atoms when the interface establishes. Therefore, ionic bonds are formed at the interface. It can be seen that the charge increases for N is more than that for C, which means the ionic bond of $\text{TiC}_{0.25}\text{N}_{0.75}$ is stronger than that of TiC one. Even though the bonding strength of both slabs is a little different, $\text{TiC}_{0.25}\text{N}_{0.75}$ as the substrate or buffer for TiC is still a promising choice.

It is not enough that the plots of charge density and charge density difference provide the qualitative analysis results for charge transfer and ionicity of the $\text{TiC}_{0.25}\text{N}_{0.75}$ (001)/TiC(001) interface configuration. Therefore, Mulliken population analysis was used to study the corresponding atoms in the interface configurations and supply the semiquantitative analysis results. The Mulliken charges on representative atoms of the selected interface are listed in Table IV. One feature is that the obtained electrons (e) from Ti to N are more than those to C, which indicates that the ionicity of $\text{TiC}_{0.25}\text{N}_{0.75}$ is higher than that of TiC. It is consistent with the above results. Moreover, the lost or gained electrons of the outermost atom ($7'$ and 7 atoms) are different from those of the bulk atoms. It can be explained that the outermost atoms have only half of the nearest neighboring electrons in comparison to the inner atoms.

In summary, the interface of TiC first terminated structure combining $\text{TiC}_{0.25}\text{N}_{0.75}$ second terminated structure is chosen to study the bonding mechanism of the $\text{TiC}_{0.25}\text{N}_{0.75}(001)/\text{TiC}(001)$ interface because all of its interface structures are stable. The interface covalent and ionic bonds of the $\text{TiC}_{0.25}\text{N}_{0.75}(001)/\text{TiC}(001)$ interface play a major role for the connection of TiC and Ti (CN) solid solution. Compared to the electronic property of the TiC(111)/TiN(111) interface,²² the ionicity of $\text{TiC}_{0.25}\text{N}_{0.75}$ is higher than that of TiC. It is evidence that doping can affect the interface properties by the amount of atom charge transfer at the interface. This indicates that doping is a practicable method to design and investigate multilayer coatings.

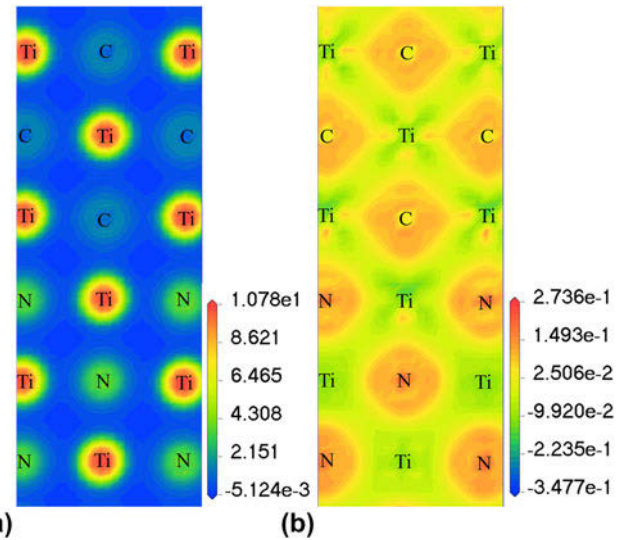


FIG. 6. Plots of (a) charge density and (b) charge density difference of the interface along the (010) plane.

TABLE IV. Mulliken charge on representative atoms of the interface.

	<i>s</i>	<i>p</i>	<i>d</i>	Total	<i>e</i>	
Ti	7'	2.27	6.39	2.58	11.24	0.76
	6'	2.12	6.57	2.60	11.29	0.71
	4'	2.12	6.59	2.61	11.32	0.68
	3'	2.12	6.59	2.61	11.31	0.69
	2'	2.12	6.59	2.61	11.31	0.69
	1'	2.11	6.58	2.62	11.30	0.70
	1	2.16	6.57	2.55	11.28	0.72
	2	2.17	6.56	2.56	11.29	0.71
	3	2.16	6.54	2.59	11.29	0.71
	6	2.15	6.51	2.61	11.27	0.73
	7	2.29	6.38	2.55	11.23	0.77
	7'	1.56	3.18	...	4.75	-0.75
	6'	1.48	3.23	...	4.71	-0.71
	4'	1.49	3.20	...	4.69	-0.69
	3'	1.49	3.20	...	4.69	-0.69
C	2'	1.48	3.20	...	4.69	-0.69
	1'	1.48	3.22	...	4.70	-0.70
	1	1.47	3.24	...	4.71	-0.71
	3	1.47	3.26	...	4.73	-0.73
	7	1.55	3.24	...	4.79	-0.79
	1	1.69	4.03	...	5.72	-0.72
	2	1.68	4.04	...	5.73	-0.73
N	3	1.68	4.04	...	5.73	-0.72
	6	1.68	4.06	...	5.74	-0.74
	7	1.73	4.04	...	5.77	-0.77

V. CONCLUSION

The interface structure of the $\text{TiC}_x\text{N}_{1-x}(001)/\text{TiC}(001)$ interface coatings was studied by first-principles calculation. To facilitate the calculation, three solid solutions with different carbon and nitrogen contents were selected, which are $\text{TiC}_{0.25}\text{N}_{0.75}$, $\text{TiC}_{0.5}\text{N}_{0.5}$, and $\text{TiC}_{0.75}\text{N}_{0.25}$, respectively. The adhesion energy is used to address the stability of the twelve interface structures of $\text{TiC}_x\text{N}_{1-x}$.

(001)/TiC(001). Therefore, the first terminated structure of TiC combining second terminated structure of $\text{TiC}_{0.25}\text{N}_{0.75}$ is chosen to study its electronic properties including PDOS, charge density, charge density difference, and Mulliken population analysis. The bonding nature of the chosen interface presents ionic and covalent characteristics, which is also existed in bulk materials. Besides, the iconicity results from that the C and N atoms gain the charge from adjacent cation atoms while the covalency is generated by the hybridization among N or C *p* states and Ti *d* states. Moreover, the extreme similarity of the PDOS between interfacial C, N, and Ti atoms and their bulk counterparts reveals that the electronic structure transition at the interface from $\text{TiC}_{0.25}\text{N}_{0.75}$ to TiC is smooth. The charge distribution is mainly around Ti, N, and C atoms. Meanwhile, the charge increased for C in TiC is less than that for N in $\text{TiC}_{0.25}\text{N}_{0.75}$, which reveals that the ionic bond in TiC is weaker than that in $\text{TiC}_{0.25}\text{N}_{0.75}$. In other words, the interface doping can affect the interface properties. And doping is a useful method to design and investigate multilayer coatings. Besides, $\text{TiC}_{0.25}\text{N}_{0.75}$ coating can be an alternative choice to combine with TiC coating in the actual production process of multilayer coatings.

ACKNOWLEDGMENT

This work was supported by the Fundamental Research Funds for the Central Universities of China (2682014CX004).

REFERENCES

- J. Kim and S. Kang: Elastic and thermo-physical properties of TiC, TiN, and their intermediate composition alloys using ab initio calculations. *J. Alloys Compd.* **528**, 20 (2012).
- G. Zhang, B. Li, B. Jiang, F. Yan, and D. Chen: Microstructure and tribological properties of TiN, TiC, and Ti(C,N) thin films prepared by closed-field unbalanced magnetron sputtering ion plating. *Appl. Surf. Sci.* **255**, 8788 (2009).
- T. Li, T. Liu, H. Wei, S. Hussain, B. Miao, W. Zeng, X. Peng, and F. Pan: Atomic and electronic structure of the TiN/MgO interface from first principles. *Comput. Mater. Sci.* **105**, 83 (2015).
- N. Liu, W. Yin, and L. Zhu: Effect of TiC/TiN powder size on microstructure and properties of Ti(C,N)-based cermets. *Mater. Sci. Eng., A* **445–446**, 707 (2007).
- J. Kim, H. Kwon, and C.W. Kwon: Temperature dependent phase stability of $\text{Ti}(\text{C}_{1-x}\text{N}_x)$ solid solutions using first-principles calculations. *Ceram. Int.* **43**, 650 (2017).
- S. Cardinal, A. Malchère, V. Garnier, and G. Fantozzi: Microstructure and mechanical properties of TiC-TiN based cermets for tools application. *Int. J. Refract. Met. Hard Mater.* **27**, 521 (2009).
- S.H. Kim, Y.J. Baik, and D. Kwon: Analysis of interfacial strengthening from composite hardness of TiN/VN and TiN/NbN multilayer hard coatings. *Surf. Coat. Technol.* **187**, 47 (2004).
- Y. Zhao, G. Lin, J. Xiao, C. Dong, and L. Wen: TiN/TiC multilayer films deposited by pulse biased arc ion plating. *Vacuum* **85**, 1 (2010).
- E.R. Parra, P.J.A. Arango, and V.J.B. Palacio: XPS structure analysis of TiN/TiC bilayers produced by pulsed vacuum arc discharge. *Dyna* **77**, 64 (2010).
- C. Liu, A. Leyland, Q. Bi, and A. Matthews: Corrosion resistance of multi-layered plasma-assisted physical vapour deposition TiN and CrN coatings. *Surf. Coat. Technol.* **141**, 164 (2001).
- M. Azadi, A.S. Rouhaghdam, S. Ahangarani, and H.H. Mofidi: Mechanical behavior of TiN/TiC multilayer coatings fabricated by plasma assisted chemical vapor deposition on AISI H13 hot work tool steel. *Surf. Coat. Technol.* **245**, 156 (2014).
- J. Zhang, Q. Xue, and S. Li: Microstructure and corrosion behavior of TiC/Ti(CN)/TiN multilayer CVD coatings on high strength steels. *Appl. Surf. Sci.* **280**, 626 (2013).
- S.K. Michelic, D. Loder, T. Reip, A.A. Barani, and C. Bernhard: Characterization of TiN, TiC, and Ti(C,N) in titanium-alloyed ferritic chromium steels focusing on the significance of different particle morphologies. *Mater. Charact.* **100**, 61 (2015).
- J.M. Lackner, W. Waldhauser, and R. Ebner: Large-area high-rate pulsed laser deposition of smooth $\text{TiC}_x\text{N}_{1-x}$ coatings at room temperature-mechanical and tribological properties. *Surf. Coat. Technol.* **188–189**, 519 (2004).
- H. Xiong, Y. Wen, X. Gan, Z. Li, and L. Chai: Influence of coarse TiCN content on the morphology and mechanical properties of ultrafine TiCN-based cermets. *Mater. Sci. Eng., A* **682**, 648 (2017).
- J. Smolik and K. Zdunek: Effect of interlayer composition on the tribological properties of TiC/Ti($\text{C}_{x}\text{N}_{1-x}$)/TiN anti-abrasive multilayer coatings. *Vacuum* **55**, 147 (1999).
- M. Yasuoka, P. Wang, and R. Murakami: Comparison of the mechanical performance of cutting tools coated by either a $\text{TiC}_x\text{N}_{1-x}$ single-layer or a TiC/Ti $\text{C}_{0.5}\text{N}_{0.5}$ /TiN multilayer using the hollow cathode discharge ion plating method. *Surf. Coat. Technol.* **206**, 2168 (2012).
- J. Zhang, Q. Xue, S. Li, and Z. Qin: Microstructure, corrosion and tribological properties of Ti(CN) multilayer coatings on 35CrMo steel by CVD. *Rare Met.* **1**, 1–7 (2014).
- X. Guo, Y. Zhang, Y. Jung, L. Li, J. Knapp, and J. Zhang: Ideal tensile strength and shear strength of $\text{ZrO}_2(111)/\text{Ni}(111)$ ceramic-metal interface: A first principle study. *Mater. Des.* **112**, 254 (2016).
- D. Yin, X. Peng, Y. Qin, and Z. Wang: Electronic property and bonding configuration at the TiN(111)/VN(111) interface. *J. Appl. Phys.* **108**, 033714 (2010).
- L.H. Liang, X.M. You, H.S. Ma, and Y.G. Wei: Interface energy and its influence on interface fracture between metal and ceramic thin films in nanoscale. *J. Appl. Phys.* **108**, 084317 (2010).
- A. Zaoui, B. Bouhafs, and P. Ruterana: First-principles calculations on the electronic structure of $\text{TiC}_x\text{N}_{1-x}$, $\text{Zr}_x\text{Nb}_{1-x}\text{C}$ and $\text{HfC}_x\text{N}_{1-x}$ alloys. *Mater. Chem. Phys.* **91**, 108 (2005).
- J. Li, Y. Yang, L. Li, J. Lou, X. Luo, and B. Huang: Interfacial properties and electronic structure of $\beta\text{-SiC}(111)/\alpha\text{-Ti}(0001)$: A first principle study. *J. Appl. Phys.* **113**, 023516 (2013).
- X. Fan, B. Chen, M. Zhang, D. Li, Z. Liu, and C. Xiao: First-principles calculations on bonding characteristic and electronic property of TiC(111)/TiN(111) interface. *Mater. Des.* **112**, 282 (2016).
- H.T. Chen and M.F. Yan: Population analysis solution to hardness enhancement in $\text{TiC}_x\text{N}_{1-x}$. *Physica B* **407**, 1183 (2012).
- S. Yi, H. Yin, J. Zheng, D.F. Khan, and X. Qu: The first-principles study on the mechanical and electronic properties about rim phase and hard phase of Ti(C,N) based cermets. *Comput. Mater. Sci.* **79**, 417 (2013).
- Y. Yang, H. Lu, C. Yu, and J.M. Chen: First-principles calculations of mechanical properties of TiC and TiN. *J. Alloys Compd.* **485**, 542 (2009).
- J. Li, Y. Yang, G. Feng, X. Luo, Q. Sun, and N. Jin: Adhesion and fracture toughness at $\alpha\text{-Ti}(0001)/\text{TiC}(111)$: A first-principles investigation. *Appl. Surf. Sci.* **286**, 240 (2013).

29. Y. Kim and B. Lee: Modified embedded-atom method interatomic potentials for the Ti–C and Ti–N binary systems. *Acta Mater.* **56**, 3481 (2008).
30. J. Yang, J. Huang, D. Fan, S. Chen, and X. Zhao: LaAlO_3 as the heterogeneous nucleus of ferrite: Experimental investigation and theoretical calculation. *J. Alloys Compd.* **683**, 357 (2016).
31. S.V. Dudy and B.I. Lundqvist: First-principles density-functional study of metal-carbonitride interface adhesion: Co/TiC(001) and Co/TiN(001). *Phys. Rev. B* **64**, 045403 (2001).
32. L. Fang, L. Wang, J. Gong, H. Dai, and D. Miao: First-principles study of bulk and (001) surface of TiC. *Trans. Nonferrous Met. Soc. China* **20**, 857 (2010).
33. J. Yang, P. Zhang, Y. Zhou, J. Guo, X. Ren, Y. Yang, and Q. Yang: First-principles study on ferrite/TiC heterogeneous nucleation interface. *J. Alloys Compd.* **556**, 160 (2013).
34. X. Zhao, X. Yuan, S. Liu, C. Zhao, C. Wang, Y. Zhou, and Q. Yang: Investigation on WC/ LaAlO_3 heterogeneous nucleation interface by first-principles. *J. Alloys Compd.* **695**, 1753 (2017).